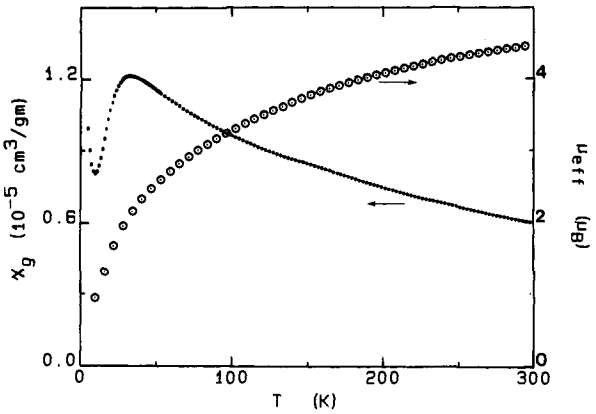

Figure 6. Plot of the magnetic susceptibility (χ_g) and effective moment (μ_{eff}) per molecule for solid II.

I at 300 K is 4.11 μ_B/molecule, indicating net antiferromagnetic exchange coupling and corresponding to 1.30 μ_B/V(IV) center. The data are distinctly nonlinear, particularly below 100 K. At high temperature, the data approach Curie–Weiss behavior, with a paramagnetic Curie temperature $\Theta = -118$ K. The effective moment of I decreases with temperature to 1.07 μ_B at 4.2 K (0.33 μ_B/V(IV) center) with a broad, shallow antiferromagnetic transition at a Néel temperature of 18 K.

The effective magnetic moment of II at 300 K is 4.49 μ_B/molecule (1.42 μ_B/V(IV) site), again indicative of antiferromagnetic coupling. At high temperatures, the data approach Curie–Weiss behavior with $\Theta = -254$ K. The magnetic susceptibility of II increases with decreasing temperature but reaches a maximum at a Néel temperature of 33 K, indicative of strong antiferromagnetic ordering.

The results are qualitatively similar to those observed by Müller et al.[3] for a series of V(IV)-containing clusters. In species with small numbers of V(IV) d^1 sites, the spins are trapped and separated resulting in spin-only values for μ_{eff}/V(IV). Spin–spin coupling increases with increasing numbers of V(IV) centers, such that μ_{eff}/μ_B per V(IV) values at room temperature for the "fully reduced" clusters $[V_{15}As_6O_{42}(H_2O)]^{6-}$ and $[H_4V_{18}O_{42}(I)]^{9-}$ are 1.08 and 1.06, respectively. The larger room temperature values observed for I and II appear to reflect the greater separation of V(IV) sites in these species (ca. 3.00–3.35 Å) compared to those observed for $[V_{15}As_6O_{42}(H_2O)]^{6-}$ and $[H_4V_{18}O_{423}(I)]^{9-}$ (ca. 2.80–3.05 Å).

Conclusions

Hydrothermal synthesis has been demonstrated to provide an effective method for the synthesis of poloxovanadium clusters incorporating conventional organic ligands. The marked cation dependence of the structures allows the isolation of species with different ligand to metal stoichiometries.

The clusters Ia and IIa exhibit the decavanadium core $\{V_{10}O_{28}\}$ with variable numbers of doubly and triply bridging oxo groups replaced by alkoxy oxygen donors of the trisalkoxy ligands. Although the clusters contain exclusively reduced V(IV) centers, the overall expansion of the $\{V_{10}O_{28}\}$ core relative to that of the V(V) parent cluster $[V_{10}O_{28}]^{6-}$ is relatively small.

Vanadium clusters appear to provide structures of sufficient flexibility to allow the existence of multiple oxidation states while retaining cluster integrity.

Acknowledgment. This work was supported by NSF Grant CHE9119910.

Supplementary Material Available: Tables of crystal data and experimental conditions for the X-ray studies of I–III atomic positional parameters, bond lengths, bond angles, and anisotropic temperature factors (60 pages); tables of calculated and observed structure factors (123 pages). Ordering information is given on any current masthead page.

H-Bonded Oxyhemoglobin Models with Substituted Picket-Fence Porphyrins: The Model Compound Equivalent of Site-Directed Mutagenesis

Gerald E. Wuenschell,[1] Catherine Tetreau,[2] Daniel Lavalette,[2] and Christopher A. Reed*,[1]

Contribution from the Department of Chemistry, University of Southern California, Los Angeles, California 90089-0744, and Unité INSERM 219, Institut Curie, Biologie, Orsay, France.
Received July 26, 1991

Abstract: Iron(II) complexes of picket-fence-type porphyrins having one of the four pivalamide pickets replaced by a substituent capable of H-bonding have been synthesized as models for oxyhemoglobin. This synthetic approach is analogous to site-directed mutagenesis of the distal residues in oxygen-binding hemoproteins. Rate and equilibrium data for dioxygen binding have been determined to evaluate the effect of the H-bonding substituent and to make comparisons with more passive substituents. The effect of H-bonding on the dioxygen affinity under standard conditions (25 °C, toluene solvent, 1,2-dimethylimidazole as axial ligand) is best illustrated by the ca. 10-fold increase observed when one pivalamide substituent of picket-fence porphyrin is replaced by a phenylurea substituent. Other substituents influence dioxygen adduct stability in a variety of ways to reveal that even with an apparently straightforward systematic approach, there can be considerable difficulty in partitioning the various factors that influence O_2 affinity. This applies to both model compounds and mutant proteins.

Introduction

The present chemical understanding of how hemoglobin functions as a reversible dioxygen carrier has arisen from an exemplary interplay of protein studies and synthetic model investigations.[3] Prominent among the synthetic models is picket-fence porphyrin.[4] Its tetrapivalamide enclosure of the dioxygen binding site mimics the distal globin wrapping in hemoglobin. Once this and other necessary and sufficient conditions for re-

(1) University of Southern California.
(2) Institut Curie.

(3) Perutz, M. F. *Annu. Rev. Biochem.* **1979**, *48*, 327.
(4) Collman, J. P. *Acc. Chem. Res.* **1977**, *10*, 265.

0002-7863/92/1514-3346$03.00/0

versible dioxygen binding were established, attention turned toward understanding how the immediate environment of the heme group controls O_2 affinity. In proteins, this can be probed by comparison of species and mutants[5] or more recently by site-directed mutagenesis.[6-9] In models, the systematic variation of the porphyrin superstructure provides a parallel approach.[10] Nevertheless, difficulties have arisen in understanding the structure/affinity relationships in both proteins and models.[11] The chemical basis for the large variation in O_2 affinity among hemoglobins remains an interesting question, particularly in trying to rationalize the high affinities found in hemoglobins from plants and from *Ascaris*.[12]

A partitioning of the distal effects on O_2 affinities into steric factors, H-bonding, environment polarity, and entropic considerations remains desirable but quite problematic. To be successful, this approach requires a good body of kinetic and thermodynamic data from systematic studies on a gradually varying series of compounds. To be legitimate, it is preferable for such studies to fit families of molecules which correlate with linear free energy relationships,[13] although such correlations may not reveal structurally explicit information. As recently pointed out,[14] there is a dearth of structural information on oxyhemoglobin models, and this weakens the connection between observable thermodynamic trends and specific structural features. Even though nearly two decades have passed since its original preparation, picket-fence porphyrin remains the only model system amenable to X-ray crystallographic study of dioxygen adducts.[15,16] For this reason, and because the wide systematic variation of one of the four pickets is synthetically feasible, we have embarked on a study of tripicket porphyrins that has the prospects of satisfying the need for both structural and thermodynamic data.

In this paper we address chiefly the synthetic aspects of the problem of H-bonding to coordinated dioxygen in tripicket derivatives.

The existence of H-bonding from distal histidine to coordinated dioxygen in oxyhemoglobin dates back to the 1964 suggestion of Pauling[17] and is now well established. Electron paramagnetic resonance (EPR)[18] and resonance Raman (RR)[19] studies on cobaltoglobins provided early support for the idea, and in 1981 a neutron diffraction study established approximate dimensions and orientations in oxymyoglobin.[20] Since then, the apparently wide variation of Fe–O–O angles observed in various oxyhemoglobins has been ascribed to differing influences of the heme pocket residues.[21,7] To date, this supposition has not been modeled in low molecular weight analogues. The high O_2 affinity of the low pH form of leghemoglobin has been ascribed to H-bonding by protonated distal histidine (i.e., imidazolium cation).[22] From pH-dependent studies the H-bond contribution is calculated to be 0.9 kcal/mol, a surprisingly low value. In hemoglobins and myoglobins at normal pH, the contribution of the distal histidine H bond (i.e., from imidazole) has been estimated to be 1–2 kcal/mol.[23]

The problem of rigorously assessing the contribution of H-bonding to the O_2 affinity of hemoglobins is the problem of removing it, by say mutation, and knowing that all other factors that influence affinity remain unchanged. Model compounds would appear to be potentially more amenable to solving this problem, but as we shall see, they too have problems in precisely partitioning the various factors that conspire to influence affinity.

Model compounds that address the H-bonding problem date back to the finding that small amounts of H-bonding solvents enhance the O_2 affinity of cobalt Schiff base complexes in dichloromethane.[24] Ironically, recent work on the vibrational coupling of $\nu_{O=O}$ to a dichloromethane solvent mode suggests that no solvent should be considered entirely innocent.[25,26] Calculations on picket-fence porphyrin suggest that the inward directing N–H of the amide dipole of a picket may contribute as much as 5–8 kcal/mol to the stability of the iron dioxygen adduct.[27] This is in qualitative agreement with the 13-fold lower affinity observed when the pivalamide substituents are replaced by nonpolar phenyl substituents[28] and the 23-fold lower affinity with ester substituents.[29] H-bonding in dioxygen adducts of cobalt tetraphenylporphyrins having a strategically placed ortho amide is implied by EPR measurements,[30] and quantitative affinities have been measured in a very useful series of naphthyl-substituted cobalt porphyrins.[31] At −42 °C an affinity increase of up to 750-fold was observed in the best case for a proximal carboxylic acid group (relative to no substituent). This is equivalent to about 3 kcal/mol stabilization. However, it should be pointed out that because of the entropic contribution to this free energy change, the value is highly temperature dependent. The affinity increase is smaller than 100-fold at −30 °C (equivalent to 2.2 kcal/mol) and, by extrapolation, is diminished to only a 2-fold effect at room temperature. In a related study, which although completely independent, is nevertheless closely related to the strategy of the present work, *decreased* cobalt–dioxygen affinities are observed when potentially H-bonding groups replace a neopentyl substituent in a modified picket-fence porphyrin.[32,33] This counterintuitive result may have an explanation in steric effects, and the researchers invoke the important concept of considering whether the energetics of *forming* the desired H bond are discounted by having to *break* a different H bond in the deoxy precursor. Recent ligand affinity data on "jellyfish"-type porphyrins reveal different responses of

(5) Dickerson, R. E.; Geis, I. *Hemoglobin*; Benjamin/Cummings: Menlo Park, CA, 1983.
(6) Nagai, K.; Luisi, B.; Shih, D.; Miyazaki, G.; Imai, K.; Poyart, C.; De Young, A.; Kwiatkowsky, L.; Noble, R. W.; Lin, S.-H.; Yu, N.-T. *Nature* **1987**, *329*, 858.
(7) Perutz, M. F.; Fermi, G.; Luisi, B.; Shaanan, B.; Liddington, R. C. *Acc. Chem. Res.* **1987**, *20*, 309.
(8) Olson, J. S.; Mathews, A. J.; Rohlfs, R. J.; Springer, B. A.; Edelberg, K. D.; Sliger, S. G.; Tame, J.; Renaud, J.-P.; Nagai, K. *Nature* **1988**, *336*, 265.
(9) Springer, B. A.; Egeberg, K. D.; Sligar, S. G.; Rohlfs, R. J.; Mathews, A. J.; Olson, J. S. *J. Biol. Chem.* **1989**, *264*, 3057.
(10) Reinert, T. J.; Suslick, K. S. *J. Chem. Educ.* **1985**, *62*, 974.
(11) Jameson, G. B.; Ibers, J. A. *Comments Inorg. Chem.* **1983**, *2*, 97.
(12) (a) Wittenberg, J. B.; Wittenberg, B. A.; Gibson, Q. H.; Trinick, M. J.; Appleby, C. A. *J. Biol. Chem.* **1986**, *261*, 13624. (b) Gibson, Q. H.; Smith, M. H. *Proc. R. Soc. London, B* **1965**, *163*, 206.
(13) Lavalette, D.; Tetreau, C.; Mispelter, J.; Momenteau, M.; Lhoste, J.-M. *Eur. J. Biochem.* **1984**, *145*, 555.
(14) Sparapany, J. W.; Crossley, M. J.; Baldwin, J. E.; Ibers, J. A. *J. Am. Chem. Soc.* **1988**, *110*, 4559.
(15) (a) Collman, J. P.; Gagne, R. R.; Reed, C. A.; Robinson, W. T.; Rodley, G. A. *Proc. Natl. Acad. Sci. U.S.A.* **1974**, *71*, 1326. (b) Jameson, G. B.; Molinaro, F. S.; Ibers, J. A.; Collman, J. P.; Brauman, J. I.; Rose, E.; Suslick, K. S. *J. Am. Chem. Soc.* **1980**, *102*, 3224.
(16) Ricard, L.; Schappacher, M.; Weiss, R.; Montiel-Montoya, R.; Bill, E.; Gonser, U.; Trautwein, A. *Nouv. J. Chim.* **1983**, *7*, 405.
(17) Pauling, L. *Nature* **1964**, *203*, 182.
(18) Ikeda-Saito, M.; Bruniori, M.; Yonetani, T. *Biochim. Biophys. Acta* **1978**, *533*, 173.
(19) Kitagawa, T.; Ondrias, M. R.; Rousseau, D. L.; Ikeda-Saito, M.; Yonetani, T. *Nature* **1982**, *298*, 869.
(20) Phillips, S. E. V.; Schoenborn, B. P. *Nature* **1981**, *292*, 81.
(21) Shaanan, B. *Nature* **1982**, *298*, 869. Shaanan, B. *J. Mol. Biol.* **1983**, *171*, 31.
(22) Appleby, C. A.; Bradbury, J. H.; Morris, R. J.; Wittenburg, B. A.; Wittenburg, J. B.; Wright, P. E. *J. Biol. Chem.* **1983**, *258*, 2254.
(23) Mino, M. P.; Porras, A. G.; Olson, J. S.; Noble, R. W.; Peterson, J. A. *J. Biol. Chem.* **1983**, *258*, 14219.
(24) Drago, R. S.; Cannady, P. J.; Leslie, K. A. *J. Am. Chem. Soc.* **1980**, *102*, 6014.
(25) Kincaid, J. R.; Proniewicz, L. M.; Bajdor, K.; Bruha, A.; Nakamoto, K. *J. Am. Chem. Soc.* **1985**, *107*, 6775.
(26) Odo, J.; Imai, H.; Kyuno, E.; Nakamoto, K. *J. Am. Chem. Soc.* **1988**, *110*, 742.
(27) Jameson, G. B.; Drago, R. S. *J. Am. Chem. Soc.* **1985**, *107*, 3017.
(28) Suslick, K. S.; Fox, M. M.; Reinert, T. J. *J. Am. Chem. Soc.* **1984**, *106*, 4522.
(29) Komatsu, T.; Hasegawa, E.; Nishide, H.; Tsuchida, E. *J. Chem. Soc., Chem. Commun.* **1990**, 66.
(30) Walker, F. A.; Bowen, J. *J. Am. Chem. Soc.* **1985**, *107*, 7632.
(31) Chang, C. K.; Kondylis, M. P. *J. Chem. Soc., Chem. Commun.* **1986**, 316.
(32) Imai, H.; Nakatsubo, A.; Nakagawa, S.; Uemori, Y.; Kyuno, E. *Synth. React. Inorg. Met-Org. Chem.* **1985**, *15*, 265.
(33) Imai, H.; Sekizawa, S.; Kyuno, E. *Inorg. Chim. Acta* **1986**, *125*, 151.

Table I. Elemental Analyses for Ligands and Complexes

compound[a]	percent C[b]	percent H[b]	percent N[b]	percent Cl[b]	percent Fe[b]
indole **3**·$^1/_3CH_2Cl_2$	74.7	5.84	11.5	2.15	
	74.4	5.91	11.1	2.44	
methoxyindole **4**·$^1/_2H_2O$	74.7	6.00	11.4		
	74.5	5.90	11.2		
benzofuran **5**·$^1/_4CH_2Cl_2$	75.0	5.77	10.3	1.62	
	74.9	5.58	10.2	1.56	
phenylurea **6**·CH_2Cl_2·$^1/_2H_2O$	70.6	5.83	11.1	6.22	
	70.7	5.91	11.0	6.36	
2-phenol **7**·$^1/_3CHCl_3$	73.3	5.78	10.3	3.26	
	73.1	5.65	10.4	3.22	
3-phenol **8**·$^1/_4CHCl_3$	73.9	5.83	10.4	2.47	
	73.7	5.81	10.5	2.55	
3-methyl-2-phenol **9**·$^1/_4CHCl_3$	74.0	5.94	10.3	2.44	
	73.8	6.07	10.09	1.96	
3,5-diacetamide **10**·$^1/_2C_5H_{12}$	73.7	6.31	11.9		
	73.6	5.98	11.5		
3,5-diacetate **11**·$^1/_4CHCl_3$	71.7	5.67	9.52	2.26	
	71.7	5.56	9.69	2.51	
3,5-methyl amide **12**·$^1/_4CHCl_3$·$3H_2O$	69.2	6.48	11.0	2.08	
	69.6	6.17	10.8	1.99	
3,5-dimethyl ester **13**	73.3	5.80	9.77	0.00	
	72.8	5.81	9.56	0.37	
Fe^{II}(indole **3**)(THF)	72.3	5.81	10.5		4.67
	72.5	5.88	10.5		4.83
Fe^{II}(methoxyindole **4**)(THF)	71.5	5.84	10.3		
	71.2	5.85	10.0		
Fe^{III}(methoxyindole **4**)(OH)·H_2O·$1/10CH_2Cl_2$)	69.3	5.57	10.5	0.59	4.66
	69.0	5.30	10.5	0.52	4.47
Fe^{II}(benzofuran **5**)(THF)	72.2	5.73	9.36		4.67
	71.9	5.86	9.36		4.58
Fe^{II}(phenylurea **6**)	72.1	5.59	11.5		5.08
	72.2	5.66	11.3		4.63
Fe^{III}(3-phenol **8**)(OH)·$1^1/_4C_7H_{16}$	72.2	6.57	9.01	0.00	4.49
	72.0	6.20	8.73	0.36	4.11
Fe^{III}(3,5-diacetamide **10**)(OH)·H_2O·$^2/_3C_7H_{16}$)	68.9	6.17	10.8	0.00	4.29
	69.3	5.73	10.3	0.25	4.81
Fe^{III}(3,5-diacetate **11**)(OH)·H_2O	68.0	5.46	9.06		4.52
	68.1	5.26	9.04		4.24
Fe^{III}(3,5-methyl amide)(OH)·H_2O	68.1	5.64	11.35		4.52
	68.0	5.61	11.13		4.23
Fe^{III}(3,5-methyl ester)(OH)·H_2O	68.0	5.46	9.06		4.52
	67.9	5.37	8.99		4.50

[a] THF = tetrahydrofuran. [b] First, second entry = calculated, found.

iron and cobalt to the same axial ligand variation.[34] This suggests caution in directly translating results from cobalt to iron.

The first success with iron porphyrins came with the nearly 10-fold higher O_2 affinity of an amide-linked basket handle porphyrin relative to its ether-linked analogue.[35] This corresponds to a stabilization of 1.3 kcal/mol at 25 °C, and structural proof that this involves the interaction of the FeO_2 moiety with the secondary amide N–H has been found in ^1H and ^{17}O NMR studies.[36,37] Related studies with an amide-containing cyclophane heme produced an even greater increase in O_2 affinity relative to nonpolar hemes.[38] In more recent work, a series of tailed hemes equipped with appended polar groups has illustrated 0.7 and 1.6 kcal/mol H-bond stabilization from an alcohol and a secondary amide, respectively.[39] In the present work, we find an effect of comparable magnitude using a picket-fence porphyrin having one of the four pivalamide pickets replaced by a phenylurea substituent. The syntheses of a variety of other tripicket porphyrins having both passive and protic replacements for the fourth picket are reported, and their superstructure conformations are explored by NMR spectroscopy. A preliminary account of the thermodynamic and kinetic features of their O_2 affinities has appeared along with a detailed review of the methodologies used to gather ligand binding data.[40]

Experimental Section

General Procedures. ^1H NMR spectra were run on JEOL FX-90Q and IBM WP-27054 instrumentation and referenced to residual protosolvent, usually chloroform or dimethyl sulfoxide. UV–vis spectra were obtained on a Shimadzu UV-260 spectrometer. Air-sensitive work was done in Schlenkware or in a Vac Atmospheres Corp. glovebox (O_2, H_2O < 0.5 ppm). Dioxygen binding parameters were obtained as previously described.[40]

Materials. *meso*-Tetrakis(*o*-aminophenyl)porphyrin was prepared in the usual manner[41,42] and the $\alpha,\alpha,\alpha,\alpha$ ("four up") isomer accumulated via the silica gel reflux process.[43,44] Poly(4-vinylpyridine) was a cross-linked material from Reilly Tar and Chemical Corp. Silica gel for column chromatography was 70–200-mesh EM 100 from Merck. 60 Pf254 (Merck 7747) was used when PLC-grade silica gel is specified. All columns were prepared as slurries. Materials were preadsorbed on a small amount and added to the top of the column in a heptane slurry. Unless otherwise indicated, all reagents and solvents were reagent-grade and used as purchased (Aldrich, Baker, Alfa). Dichloromethane and

(34) Uemori, E.; Kyuno, E. *Inorg. Chem.* **1989**, *28*, 1690.
(35) Momenteau, M.; Lavalette, D. *J. Chem. Soc., Chem. Commun.* **1982**, 341.
(36) Mispelter, M.; Momenteau, M.; Lavalette, D.; Lhoste, J.-M. *J. Am. Chem. Soc.* **1983**, *105*, 5165.
(37) Gerothanassis, I. P.; Momenteau, M.; Loock, B. *J. Am. Chem. Soc.* **1989**, *111*, 7006.
(38) Traylor, T. G.; Koga, N.; Deardruff, L. A. *J. Am. Chem. Soc.* **1985**, *107*, 6504.
(39) Chang, C. K.; Ward, B.; Young, R.; Kondylis, M. P. *J. Macromol. Sci., Chem.* **1988**, *A25*, 1307.
(40) Lavalette, D.; Tetreau, C.; Momenteau, M.; Mispelter, J.; Lhoste, J. M.; Wuenschell, G. E.; Reed, C. A. *Laser Chem.* **1990**, *10*, 297.
(41) Collman, J. P.; Gagne, R. R.; Reed, C. A.; Halbert, T. R.; Lang, G.; Robinson, W. T. *J. Am. Chem. Soc.* **1975**, *97*, 1427.
(42) Sorrell, T. N. *Inorg. Synth.* **1980**, *20*, 161.
(43) Lindsey, J. *J. Org. Chem.* **1980**, *45*, 5215.
(44) Elliott, C. M. *Anal. Chem.* **1980**, *52*, 666.

pyridine were dried over molecular sieves (4A) for several days. Thionyl chloride was distilled from triphenyl phosphite. Tetrahydrofuran, toluene, and heptane were distilled from sodium/benzophenone for glovebox use. Other solvents were deoxygenated by bubbling with inert gas. Alumina (neutral, column grade) was degassed by heating to 100 °C under vacuum and deactivated in the glovebox by treatment with 10 mL of water/100 g of alumina. Elemental analyses are given in Table I.

***meso*-Tris(α,α,α-*o*-aminophenyl)mono[α-*o*-[(triphenylmethyl)-amino]phenyl]porphyrin (Monotrityl 1).** *meso*-Tetrakis(α,α,α,α-*o*-aminophenyl)porphyrin (2.1 g, 3.1 mmol) and poly(4-vinylpyridine) (10 g, 85 mequiv were added to dry dichloromethane (200 mL) and cooled to ice temperature. Triphenylmethyl bromide (1.05 g, 3.25 mmol) in dry dichloromethane was added dropwise, with stirring, over 1 h. The mixture was then stirred with 10% aqueous ammonia (200 mL) and filtered to remove the polymeric base. The dichloromethane layer was separated, washed again with ammonia followed twice by water, dried over sodium sulfate, and evaporated to dryness on a rotary evaporator. Chromatography was done by preadsorption of a dichloromethane solution onto a small amount of silica gel, loading onto a 40-mm-diameter column wet-packed with about 400 mL (dry volume) of silica gel. Elution with 9:1 hexanes/ethyl/acetate gave band 1, an 8:2 mixture gave band 2, a 7:3 mixture gave band 3, and acetone gave a fourth and final band. Band 1 was shown by TLC and ^{1}H NMR[45] to be a mixture of mono(α-*o*-aminophenyl)tris[α,α,α-*o*-[(triphenylmethyl)amino]phenyl]porphyrin (tritrityl) and 5,15-bis(α,α-*o*-aminophenyl)-10,20-bis[α,α-*o*-[(triphenylmethyl)amino]phenyl]porphyrin (*trans*-ditrityl), band 2 was *cis*-ditrityl, band 4 was recovered starting material, and band 3 was the desired monotrityl.[46] This was recrystallized from dichloromethane/hexanes to give a purple crystalline product (1.5 g, 53%). Fractions 1 (0.25 g, ca. 6%) and 2 (0.45 g, 13%) were detritylated using trichloroacetic acid in dichloromethane and combined with fraction 4 (0.51 g, 24%) to give a total porphyrin recovery of ca. 96%.

A similar preparation of **1** using potassium carbonate or pyridine as base instead of poly(vinylpyridine) gave similar results but with slightly lower yield (47%).

***meso*-Mono(α-*o*-aminophenyl)tris(α,α,α-*o*-pivalamidophenyl)-porphyrin (Tripicket 2).** Monotrityl **1** (4.9 g, 5.34 mmol) was dissolved in dry dichloromethane (200 mL) and an approximately equal amount of anhydrous potassium carbonate added. After cooling under dry nitrogen to 0 °C, pivaloyl chloride (12 mL, 32.5 mmol) was added and the mixture stirred for 3 h. The reaction mixture was washed once each with water, 1 M hydrochloride acid, and 10% aqueous ammonia and again with water (500-mL volumes). The solution was dried over sodium sulfate, filtered, and evaporated to dryness to give an intermediate presumed to be tris(α,α,α-*o*-pivalamidophenyl)mono[α-*o*-[(triphenylmethyl)amino]phenyl]porphyrin (tripicket–monotrityl). This intermediate was dissolved in dry dichloromethane (200 mL) and cooled to 0 °C, and trichloroacetic acid (12 g, 73.4 mmol) was added. The reaction mixture was then washed with water, with three aliquots of 10% aqueous ammonia, and finally twice with water before drying over sodium sulfate, filtering, and evaporating on a rotary evaporator. Chromatography on silica gel (30 cm × 70 mm diameter) with 6:1:1 chloroform/hexanes/diethyl ether allowed removal of minor impurities which eluted early. The product was collected as the major band once TLC monitoring showed it to be free of impurities. Recrystallization from dichloromethane/methanol gave purple crystals which were vacuum dried (4.1 g, 83%). The ^{1}H NMR spectrum is shown in Figure S1 of the supplementary material.

***meso*-Mono[α-*o*-(2-indolecarboxamido)phenyl]tris(α,α,α-*o*-pivalamidophenyl)porphyrin (Tripicket–Indole 3).** A slurry of indole-2-carboxylic acid (0.5 g, 3.1 mmol) in dry dichloromethane (25 mL) was treated with thionyl chloride (0.20 mL, 2.7 mmol) and dimethylformamide (8 drops). Within a few minutes the reaction mixture turned yellow; after several hours, the acid had all dissolved, and the deep yellow solution was stirred for 24 h. After cooling to 0 °C, tripicket **2** (0.50 g, 0.54 mmol) was added, giving a dark green solution. Dry pyridine was added dropwise until the solution turned red (ca. 8 drops), and then an additional 50% of that volume was added (ca. 12 drops total). The starting material and product were found to be essentially inseparable by TLC, but the reaction could be monitored by the pink fluorescence of the product on TLC under long-wavelength UV light. After 7 h the reaction mixture was washed with saturated potassium carbonate, with 1 M hydrochloric acid, twice with saturated potassium carbonate, and twice with water before drying over sodium sulfate, filtering, and evaporating to dryness on a rotary evaporator. Flash chromatography was performed with PLC-grade silica gel with ca. 10 psi of pressure, eluting with 4% methanol in chloroform. The single major band was collected, the solvent evaporated under reduced pressure, and the product recrystallized from dichloromethane/heptane (0.54 g, 93%). The ^{1}H NMR spectrum is shown in Figure S2 of the supplementary material.

***meso*-Mono[α-*o*-(5-methoxyindole-2-carboxamido)phenyl]tris(α,α,α-*o*-pivalamidophenyl)porphyrin (Tripicket–5-Methoxyindole 4).** This was prepared from 5-methoxyindole-2-carboxylic acid (13.5 mmol) and **2** (1.1 mmol) in a manner similar to that for **3** except that the reaction time was only 1 h and 4:3:3 chloroform/hexanes/diethyl ether was used for the chromatographic eluent, taking a middle cut of the eluate (82%). The ^{1}H NMR spectrum is shown in Figure S3 of the supplementary material.

***meso*-Mono[α-*o*-(2-benzofurancarboxamido)phenyl]tris(α,α,α-*o*-pivalamidophenyl)porphyrin (Tripicket–Benzofuran 5).** This was prepared from benzofuran-2-carboxylic acid (1.7 mmol) and tripicket **2** (0.27 mmol) in a manner similar to that for **4** and isolated in 81% yield. The ^{1}H NMR spectrum is shown in Figure S4 of the supplementary material.

***meso*-Mono[α-*o*-(phenylcarbamido)phenyl]tris(α,α,α-*o*-pivalamidophenyl)porphyrin (Tripicket–Phenylurea 6).** Phenyl isocyanate (0.50 mL, 4.6 mmol) and tripicket **2** (0.50 g, 0.54 mmol) were stirred in dry dichloromethane (10 mL) at 0 °C overnight. The product was chromatographed on silica gel eluting with 6:1:1 chloroform/hexanes/diethyl ether, taking a middle cut. In order to remove a colorless UV-active impurity, the product was rechromatographed on PLC-grade silica gel eluting first with 3:2 diethyl ether/hexanes (500 mL), then with 4:1 diethyl ether/hexanes (500 mL), and finally with 6:1:1 chloroform/hexanes/diethyl ether, taking a middle cut. Evaporation to dryness gave a purple solid (0.30 g, 53%) which was recrystallized for analysis from dichloromethane/heptane/pentane. The ^{1}H NMR spectrum is shown in Figure S5 of the supplementary material.

***meso*-Mono[α-*o*-(2-hydroxybenzenecarboxamido)phenyl]tris(α,α,α-*o*-pivalamidophenyl)porphyrin (Tripicket–2-Phenol 7).** Acetylsalicylic acid (0.17 g, 0.96 mmol) was converted to the acid chloride in a manner similar to that used for **3** and the acetyl derivative of the desired product isolated by evaporation of solvent under reduced pressure. It was then dissolved in tetrahydrofuran (10 mL) and methanol (5 mL) and deacylated by treatment with potassium carbonate (1 g) in water (10 mL) over 4 h. The product was extracted into dichloromethane (20 mL) by the addition of water (200 mL), using gentle mixing to avoid emulsification. The dichloromethane layer was washed twice with water and dried by filtration through a layer of potassium carbonate. Several minor components were removed by chromatography on PLC-grade silica gel eluting with 4:3:3 chloroform/hexanes/diethyl ether. The product was isolated as a purple solid by removal of solvents under vacuum and reevaporation from chloroform/heptane/pentane (0.037 g, 61%). The ^{1}H NMR spectrum is shown in Figure S6 of the supplementary material.

***meso*-Mono[α-*o*-(3-hydroxybenzenecarboxamido)phenyl]tris(α,α,α-*o*-pivalamidophenyl)porphyrin (Tripicket–3-Phenol 8).** 3-Acetylbenzoic acid was prepared by treatment of 3-hydroxybenzoic acid (10 g, 72.4 mmol) with acetyl chloride (6 mL, 84.4 mmol) in diethyl ether (100 mL) and pyridine (6 mL) overnight. Water (15 mL) was added, and upon removal of the ether on a rotary evaporator, the oil was crystallized. This was recrystallized from hot water and dried under vacuum (4.4 g, 34%). The desired tripicket–3-phenol **8** was prepared in a manner identical to that for **7** using 3-acetylbenzoic acid (0.16 g, 0.89 mmol) and tripicket **2** (0.055 g, 0.059 mmol) to give 0.033 g of the product (54%). The ^{1}H NMR spectrum is shown in Figure S7 of the supplementary material.

***meso*-Mono[α-*o*-(2-hydroxy-3-methylbenzenecarboxamido)phenyl]-tris(α,α,α-*o*-pivalamidophenyl)porphyrin (Tripicket–3-Methyl-2-phenol 9).** This was prepared from 3-methylsalicylic acid in a manner identical to that for **8** using 2-acetyl-3-methylbenzoic acid (0.16 g, 0.82 mmol) and **2** (0.054 g, 0.059 mmol) to give 0.037 g of product (59%) from chloroform/heptane/pentane. The ^{1}H NMR spectrum is shown in Figure S8 of the supplementary material.

***meso*-Mono[α-*o*-(3,5-diacetamidobenzenecarboxamido)phenyl]tris-(α,α,α-*o*-pivalamidophenyl)porphyrin (Tripicket–3,5-Diacetamide 10).** A slurry of 3,5-diaminobenzoic acid (5.8 g, 38 mmol) in diethyl ether (75 mL) at 0 °C was treated with acetyl chloride (10 mL, 140 mmol) in diethyl ether (10 mL). A solution of pyridine (10 mL) in diethyl ether (10 mL) was added cautiously over a period of 1 h. After 1 h of stirring, the reaction was quenched with ethanol (10 mL) and the solvents were stripped to an oil. Water (100 mL) was added, causing the formation of a grey precipitate that was collected by paper filtration, washed with water and then 0.5 M hydrochloric acid to remove an oily residue, and dried under vacuum (6.6 g, 73%). The 3,5-diacetamidobenzoic acid (1.5 g, 6.4 mmol) in dry dichloromethane (25 mL) and dimethylformamide (2 mL) was treated with thionyl chloride (0.9 mL, 12 mmol) and stirred for 24 h. A portion of the resulting 3,5-diacetamidobenzoyl chloride

(45) Larsen, N. G.; Boyd, P. D. W. D.; Rodgers, S. J.; Wuenschell, G. E.; Koch, C. A.; Rasmussen, S.; Tate, J. R.; Erler, B. S.; Reed, C. A. *J. Am. Chem. Soc.* **1986**, *108*, 6950.

(46) Collman, J. P.; Brauman, J. I.; Collins, T. J.; Iverson, B.; Lang, G.; Peltman, R. B.; Sessler, J. L.; Walters, M. A. *J. Am. Chem. Soc.* **1983**, *105*, 3038.

solution (30 mL) was added to tripicket **2** (0.295 g, 0.318 mmol) followed by pyridine (2.5 mL), and after 1 h the product was worked up in a manner similar to that described for **7** to give 0.20 g of product (55%). The ^{1}H NMR spectrum is shown in Figure S9 of the supplementary material.

***meso*-Mono[α-*o*-(3,5-diacetylbenzenecarboxamido)phenyl]tris(α,α,α-*o*-pivalamidophenyl)porphyrin (Tripicket-3,5-Diacetate 11).** This was prepared from 3,5-dihydroxybenzoic acid by methods similar to those described for **10**. Recrystallization from chloroform/heptane gave purple crystals (93%). The ^{1}H NMR spectrum is shown in Figure S10 of the supplementary material.

***meso*-Mono[α-*o*-[3,5-bis(methylcarbamoyl)benzenecarboxamido]-phenyl]tris(α,α,*o*-pivalamidophenyl)porphyrin (Tripicket-3,5-Methyl Amide 12).** 1,3,5-Benzenetricarbonyl trichloride (1.3 g, 4.9 mmol) in dry dichloromethane (25 mL) and pyridine (1.5 mL) was treated with tripicket **2** (0.18 g, 0.19 mmol) in dry dichloromethane dropwise over 1 h. Monomethylamine was bubbled through the cooled solution for 20 min. Workup involved washing three times with water, once with 1 M hydrochloric acid, and then sequentially with water, saturated potassium carbonate, saturated potassium chloride, and water. The solution was dried by filtering through a layer of anhydrous sodium sulfate and evaporated on a rotary evaporator. Chromatography on PLC-grade silica gel with 4% methanol in chloroform gave a middle cut of pure product (0.18 g, 78%) which was recrystallized for analysis from chloroform/heptane/pentane. The ^{1}H NMR spectrum is shown in Figure S11 of the supplementary material.

***meso*-Mono[α-*o*-[3,5-bis[(methyloxy)carbonyl]benzenecarboxamido)-phenyl]tris(α,α,α-*o*-pivalamidophenyl)porphyrin (Tripicket-3,5-Methyl Ester 13).** This was prepared in a manner similar to that for **13** from 1,3,5-benzenetricarbonyl trichloride (1.18 g, 4.46 mmol) and tripicket **2** (0.11 g, 0.12 mmol) in dry dichloromethane with subsequent esterification with dry methanol. Evaporation, extraction into dichloromethane, addition of powdered K_2CO_3, and flash chromatography on PLC-grade silica gel eluting with 4:3:3 chloroform/hexanes/diethyl ether gave pure product (0.11 g, 82%). The ^{1}H NMR spectrum is shown in Figure S12 of the supplementary material.

Iron Insertion. All porphyrins were metalated by a similar procedure. In a typical experiment, ligand (100 mg) and anhydrous potassium carbonate (75 mg) were weighed into a flask and taken into the glovebox. Ferrous bromide (100 mg) was added, followed by toluene (10 mL) and tetrahydrofuran (10 mL). After stirring for 2 days, the reaction mixture was filtered, reduced to about 50% volume under vacuum, and filtered through a 20-mL buret-sized column of silica gel. Tetrahydrofuran/toluene mixtures were used as eluent, the amount of tetrahydrofuran being just enough to elute the iron(II) porphyrin. To ensure that the eluted product was not contaminated with ferrous bromide, the spent column was exposed to air. A yellow band soon appeared, revealing the extent of ferrous bromide elution. If the column showed possible elution of ferrous bromide, the product was rechromatographed. Alumina was found to adsorb ferrous bromide better than silica gel, but some porphyrin decomposition was frequently detected. The eluent was usually evaporated to dryness under vacuum and the product taken up in a very small amount of tetrahydrofuran, filtered through a fine frit, and crystallized by heptane diffusion. Little attempt was made to optimize yields, but 45–80% isolated yields were typical. Significant deviations from the general procedure are noted as follows. The elution of the metalated complex from the 2-phenol **7** required 5 drops of acetic acid in tetrahydrofuran, and redissolution required 7:3 tetrahydrofuran/methanol. The product is apparently polymeric but does dissolve in tetrahydrofuran in the presence of imidazoles. The complex from the 3-phenol **8** was worked up aerobically. The complex from the 3-methyl-2-phenol **9** required 7:3 tetrahydrofuran/methanol for elution from alumina. The complex from the 3,5-methyl ester **13** required a second metalation with iron(II) bromide to get complete insertion.

All complexes were characterized by UV–vis spectroscopy in toluene and by elemental analysis, sometimes as the aerobically worked-up iron(III) hydroxo and/or μ-oxo complexes. Iron(II) complexes of ligands **3**, **4**, **6**, **10**, and **13** showed typical four-coordinate spectra: λ_{max} 415–418 (Soret), 441–444 (Soret), and 535–538 (α,β) nm. Those of the 3,5-diacetate **11** and the 3,5-methyl amide **12** showed more typically five-coordinate spectra: λ_{max} 425–432 (Soret), 536–537 (β), and 561–562 (α) nm. All iron(II) complexes gave typical five-coordinate spectra in the presence of 1,2-dimethylimidazole: λ_{max} 430–435 (Soret), 530–535 (shoulder except with **11** and **12**) (β), and 555–565 (α) nm. All iron(II) species air-oxidized eventually to typical[45] hydroxy- or μ-oxoiron(III) species: λ_{max} 418–425 (Soret), 570–575 (β), and 610 (sh) (α) nm. Analytical data are listed in Table I. The iron(III) complexes are formulated as hydroxy species but are analytically indistinguishable from μ-oxo dimers with water of solvation. As discussed previously,[45] these alternate formulations are spectroscopically difficult to distinguish and may in fact be mixtures. The choice of which compounds were analyzed was based mainly on availability of microcrystalline product. Spectral criteria were used for compound identification in cases where analytical data were not obtained.

Discussion

Synthesis. The purpose of this investigation was to synthesize a series of closely related oxyhemoglobin models whose differing distal effects would be reflected rationally in their differing dioxygen affinities and on/off binding rates. The strategy was to systematically replace one of the four pivalamide substituents of picket-fence porphyrin with groups of varying polarity, steric influence, and H-bonding capability. Picket-fence porphyrin was chosen for baseline comparison because of synthetic feasibility, convenient solubility, and the uniqueness of this system to yield dioxygen complexes for X-ray structure determination. The replacements which have been achieved synthetically to date are illustrated in Figure 1. They include the indole **3** having an N–H group in the superstructure that is potentially capable of H-bonding to coordinated dioxygen, a 5-methoxyindole variant **4** and the benzofuran analogue **5**. The benzofuran was chosen as an isostructural analogue of the indole, but one which is incapable of H-bonding. The phenylurea **6** positions an N–H moiety in a location different from that of the indole **3** and enjoys the advantage of predictable orientation and planarity of the urea linkage. The three phenol-containing porphyrins **7–9** provide quite acidic functionality in the superstructure. The 3,5-diacetamide **10** and the 3,5-methyl amide **12** were chosen to position amide functionality over the $Fe(O_2)$ binding site in two slightly different ways. By having 3,5-*di*substitution we hoped to avoid any uncertainty about whether the amide was directed inward toward the center of the porphyrin ring or outward away from the $Fe(O_2)$ moiety. (As we will show below, the latter situation obtains in the indole **3**.) Finally, the 3,5-diacetate **11** and the 3,5-dimethyl ester **13** were prepared as non-H-bonding analogues of the two 3,5-amides **10** and **12** having very similar steric properties but diminished polarity. In all cases the distal functionality is linked to the porphyrin via amide functionality so as to preserve identity with picket-fence porphyrin. This was considered important for making valid comparisons because the amide dipole is known to contribute to the O_2 affinity.[27-29]

The syntheses of the functionalized tripicket ligands **3–13** were all based on amide coupling methods. An improvement in the synthesis of the tripicket–monoamino precursor **2** was made by tritylating the four-up amino porphyrin **1** prior to acylating with pivaloyl chloride. This not only improves the one-batch yield from 34%[41] to 53% but allows easy recovery of over-tritylated precursor, via acid cleavage, to give reusable **1** in significant amounts. Another improvement arises from the use of poly(vinylpyridine) as a base for the acylation instead of pyridine. This makes the workup less vulnerable to persistent pyridine.

Concurrent with the present work, Imai et al. reported the synthesis of a number of closely related porphyrins based on a neopentyl amide tripicket motif.[32] The fourth picket included amide-linked primary amides, α-methanol, 2-phenol, and a selection of less polar substituents.[33] There is overlap between the two studies only in the case of the 2-phenol substituent.

To date we have been unsuccessful in coupling the highly desirable imidazole-2-carboxamide or benzimidazole-2-carboxamide substituent as the fourth picket. This would, of course, mimic the distal histidine of hemoglobin much better than the secondary amides, urea, and indole functionalities that we have been able to append. However, this need has become less urgent with the recognition (see below) that H-bonding of such an imidazole to its own connecting amide is probable. This would have the effect of directing the N–H bond outward, i.e., exo to the center of the porphyrin ring, making it less available for H-bonding to the FeO_2 moiety.

Ligand Structure. Our need for structural information about the conformation of the appended substituents led us to an extensive investigation of the ^{1}H NMR spectra of the free ligands. Our earlier investigation of "pincer porphyrin" had uncovered important interpicket H-bonding interactions, and in addition,

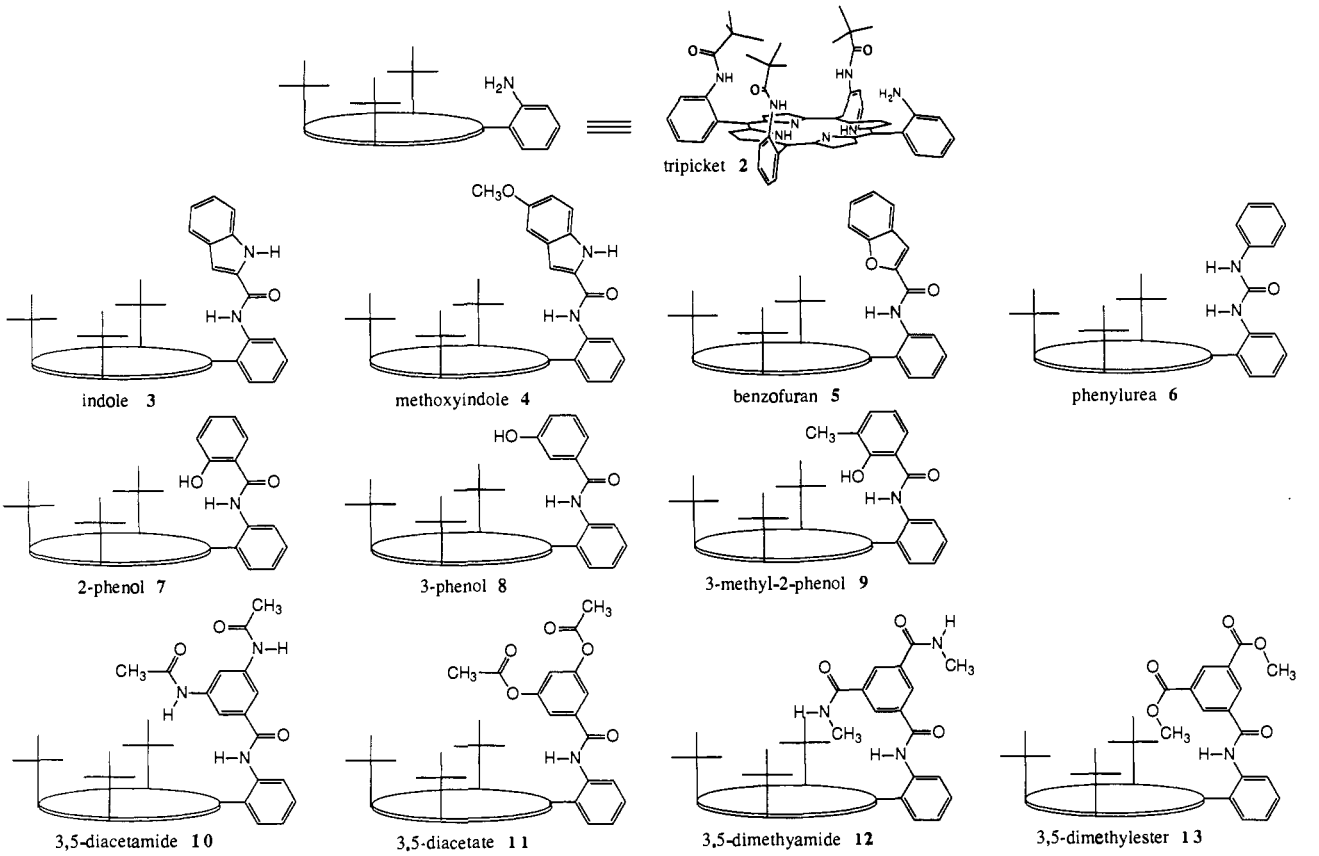

Figure 1. Schematic representations of the 11 new ligands **3–13** and precursor **2**.

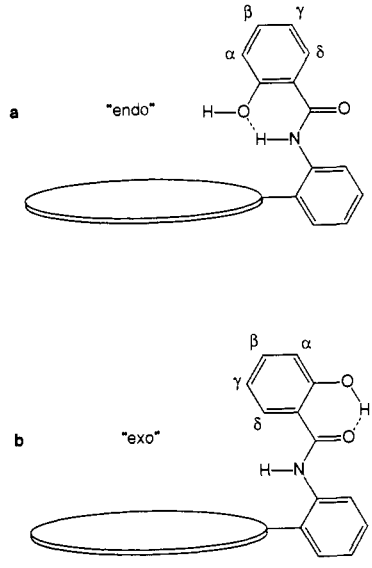

Figure 2. The two possible conformations for the phenol group of the tripicket–2-phenol ligand **7**.

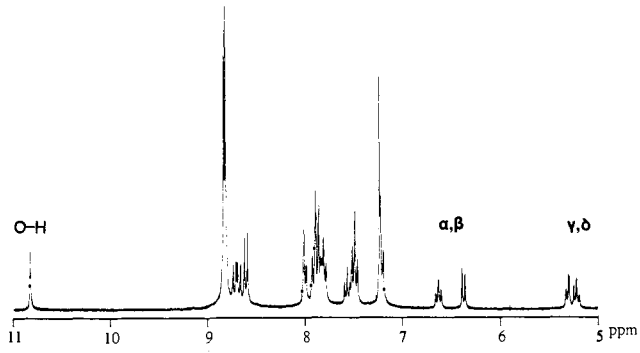

Figure 3. The downfield portion of the 270-MHz ^{1}H NMR spectrum of the 2-phenol ligand **7**.

porphyrin ring current effects were shown to be very useful in determining appendage orientation.[45] Illustrative of the structural possibilities in the present work is the case of the 2-phenol ligand **7** where two major conformations can be envisaged depending upon the connectivity of cyclic H-bond formation. Figure 2 illustrates (a) the desirable configuration with the O–H endo to the porphyrin ring and (b) the undesirable exo-oriented structure. Both contain H-bonding in six-membered rings, and the stronger would be expected to hold the structure in a single rigid configuration. Structure a is expected to have a phenolic resonance strongly upfield shifted due to its location over the porphyrin ring current. In addition, two of the arene protons (α and β) should experience moderate upfield shifts. By contrast, structure b should have a downfield-shifted phenolic resonance due to H-bonding and possible deshielding ring current effects from its location at the periphery of both the porphyrin and the substituent arene rings. In addition, two of the arene resonances (γ and δ) should experience strong upfield shifts from the porphyrin ring current. The observed spectrum, illustrated in Figure 3, clearly conforms to that of configuration b. The upfield singlet at 10.85 ppm was confirmed as the phenolic proton by its disappearance upon addition of D_2O. The strongly upfield-shifted resonances at 5.2 and 5.3 must arise from the γ and δ protons. These assignments are corroborated by the spectrum of the closely related 3-methyl-2-phenol ligand **9** whose phenolic proton is again strongly shifted downfield (to 12.0 ppm) and whose arene protons are spread out between 4.5 and 7.0 ppm. In addition, the methyl group resonance appears at the relatively unaffected value of 1.9 ppm. If the more desirable endo configuration were present, a strong upfield shift of this methyl resonance would be expected, because of its orientation over the porphyrin ring.

This finding of exo H-bonding in the 2-phenol ligands led us to suspect the same in the indole ligands **3** and **4**. Of the endo and exo configurations, the H-bonding in the six-membered ring of the exo (see Figure 4) is likely to be the exclusive configuration since in the free-base ligand there is no H-bonding to O_2 to stabilize

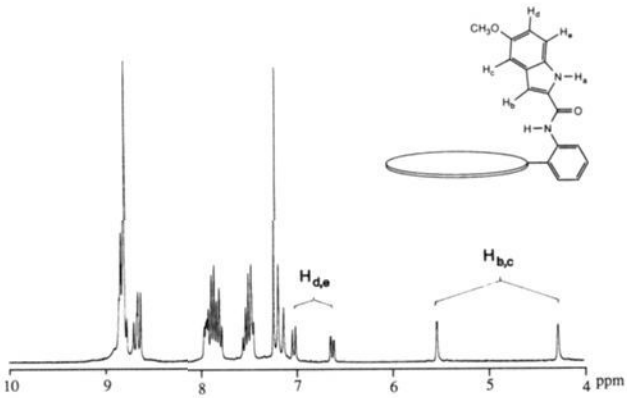

Figure 4. The downfield portion of the 270-MHz ^{1}H NMR spectrum of the 5-methoxyindole ligand **4** and a partial assignment of the signals.

the desired inward-directed N–H configuration. The indole ligand **3** presents special problems for ^{1}H NMR analysis. It has a pseudo-C_2 axis of symmetry around the 2-carboxamide linkage, and in addition, the low acidity of the N–H proton makes exchange with D_2O quite slow. On the other hand, the 5-methoxyindole ligand **4** has a readily interpretable spectrum. As illustrated in Figure 4, the appearance of uncoupled singlets at the markedly upfield positions of 4.3 and 5.5 ppm is strongly indicative of an exo configuration. The N–H_a resonance, expected to be broader than the C–H resonances, was not immediately assignable but was presumed to occur in the 7–9 ppm region. Deuterium NMR on a sample of the indole ligand **3** that had been carefully equilibrated with D_2O and dried with D_2O-cycled molecular sieves revealed a broad singlet at 9.2 ppm assignable to the indole N–D. This resonance was absent from a similarly treated sample of the benzofuran **5** which showed broad signals at 7.5–8.0 and 2.5 assignable to the four amide and two porphyrinic N–D resonances, respectively. The position of the indole N–D resonance at 9.2 ppm is inconsistent with an endo structure since an upfield shift of as much as 2–3 ppm might be expected if the N–H moiety was positioned over the porphyrin ring. It appears in the ^{1}H spectrum of **3** as a relatively broad resonance at 9.0 ppm.

The benzofuran ligand **5** has a ^{1}H NMR spectrum that is nearly identical to that of the indole ligand **3** except that there is only one substituent resonance upfield of 6 ppm, a doublet at 4.8 ppm with integrated intensity equivalent to one proton. Since the indole **3** has two such resonances, a doublet at 6.0 and a singlet at 4.15 ppm, it is probable that the benzofuran O atom is directed inward toward the center of the porphyrin ring. If directed outward, a second, markedly upfield-shifted resonance would be expected from the arene proton in the 3-position of the five-membered ring.

The conformation of the phenylurea ligand **6** is best discussed by shifting the point of focus from the effect of the porphyrin ring current on the substituent resonances to that of the substituent ring currents on the pivaloyl pickets. All of the ligands synthesized in this study have appended aryl groups which, as a consequence of near van der Waals contact with two adjacent (cis) pickets, can exert substantial ring current shifts on these *tert*-butyl ^{1}H resonances. The direction of the shift will depend on the relative disposition of the average *tert*-butyl proton position and the shielding and deshielding zones of the arene substituent. Figure 5 shows the ^{1}H NMR signal for the *tert*-butyl groups of three ligands: the indole **3**, the 2-phenol **7**, and the phenylurea **6**. The two singlets in each spectrum appear in a 2:1 ratio corresponding to the cis/trans substitution pattern of *tert*-butyl groups on the porphyrin ring. Alongside each spectrum is a drawing which illustrates the relationship between the *tert*-butyl protons (shaded area) and the ring-current boundaries (±) calculated for benzene[47] and positioned according to functional group attachment with standard bonding parameters. Immediately obvious from the three spectra is that the resonances of the unique (i.e., trans) *tert*-butyl

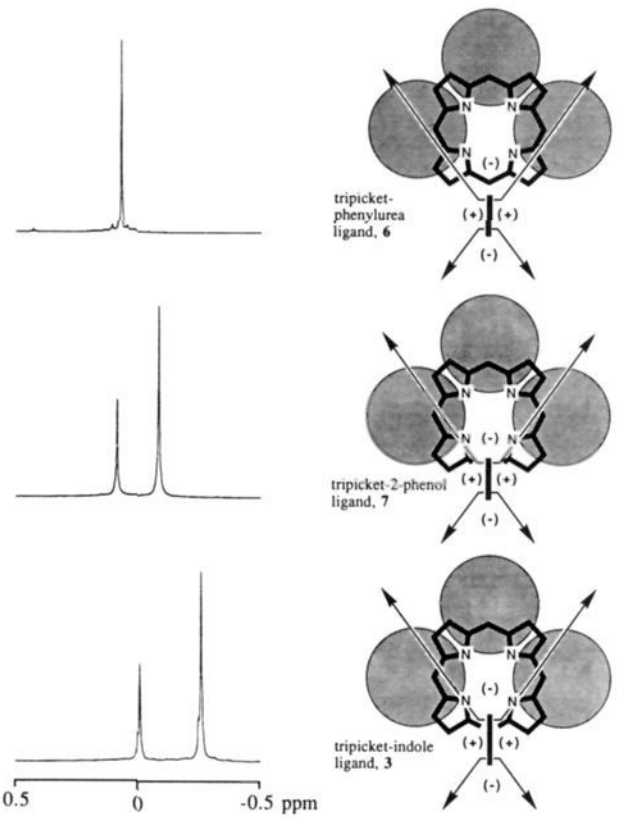

Figure 5. ^{1}H NMR signals for the *tert*-butyl groups of three representative ligands and the ring current effects influencing their chemical shifts. The shaded circles represent the *tert*-butyl groups. The arrows mark the boundaries for upfield (+) and downfield (−) ring current effects from the substituted arene.

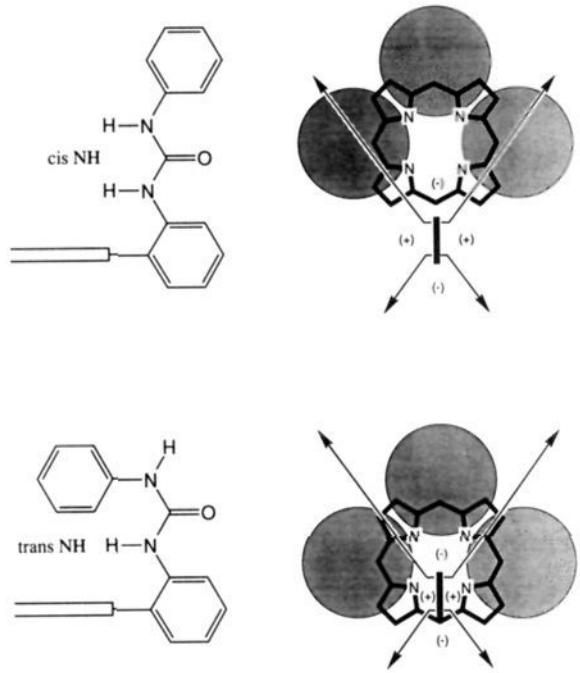

Figure 6. Two possible conformations of the phenylurea ligand **6** and their corresponding ring current effects generated by the phenyl group.

groups remain relatively unaffected. However, the degenerate, cis *tert*-butyl groups experience a significant upfield shift in the case of the indole and 2-phenol ligands, as predicted by the accompanying influence diagrams. By contrast, the cis *tert*-butyl resonances of the phenylurea ligand experience no significant shift. Thus, the urea phenyl group is relatively remote from the pivalamides and/or its ring current boundary bisects the *tert*-butyl

(47) Becker, E. D. *High Resolution NMR: Theory and Chemical Applications*; Academic: New York, 1980; pp 73–74.

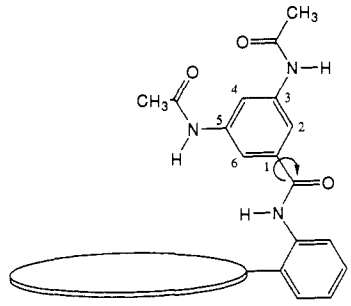

Figure 7. A possible orientation of the 3,5-diacetamidophenyl group of ligand **10** and the rotation required to give equivalence to the methyl groups.

group, leading to canceling positive and negative effects. Both conditions probably contribute. The two alternative configurations are illustrated in Figure 6. The lower diagram has a transoid arrangement of N–H groups in the urea linkage and projects the phenyl substituent sharply toward the center of the porphyrin ring. The ring-current boundary diagram predicts a strong upfield shift which is not seen. The more normal, cis relationship to the N–H groups in the upper diagram projects the phenyl group to a more remote position, and the ring-current boundaries show inconsequential bias. Thus, the upper conformation of Figure 6 must exist in the phenylurea ligand, consistent with original design. The upper N–H is well placed for H-bonding to $Fe(O_2)$ in the central cavity and is probably prepositioned in a planar array. By contrast, the N–H group of the indole ligand **3** is directed outward (Figure 4) and is tied up with H-bonding to its own connecting amide. Thus, for the purposes of this project, the indole ligand is useful only as a steric substitution unless, of course, H-bonding to an $Fe(O_2)$ moiety is stronger than to its own amide.

The free-base ^{1}H NMR spectrum of the 3-phenol ligand **8** is less informative with regard to superstructure conformation. The signals are broader than in the exo-oriented 2-phenol **7** suggestive of conformational flexibility although the upfield shifts of the phenol aryl protons do confirm substituent positioning in the expected position over the porphyrin ring. We were unable to assign the phenolic O–H resonance which again suggests a lack of conformational rigidity.

The remaining ligands **10–13** were designed with 3,5-substituted phenyl groups so that their inward or outward positioning would be inconsequential.[48] This is illustrated in Figure 7 for the diacetamide ligand **10**. The low-temperature ^{1}H NMR spectrum (220 K) is perhaps consistent with this orientation although not uniquely so. It shows methyl group singlets at 1.5 ppm (assigned to the 3-position) and 0.0 ppm (assigned to the 5-position and somewhat upfield shifted due to the porphyrin ring current). As the sample is warmed these signals diminish in unison, and at room temperature they vanish. At 333 K a broad peak at 1.3 ppm may correspond to their time-averaged signal, the result of rotation around the amide linkage indicated in Figure 7. The complication in this explanation is that *four* signals are seen in the *tert*-butyl region at low temperature and quite complex changes occur in this and other parts of the spectrum up to about 330 K, above which a singlet is observed for the *tert*-butyl groups at 270 MHz. Three additional fluxional processes may be occurring, some of which have been discussed by Odo et al.[49] The first is N–H tautomerism of the inner porphyrin core. This is known to occur in tetraphenylporphyrin[50] with a free energy of 11.6 kcal/mol, making it a very likely component of the fluxionality of **10** in the temperature range explored. The second is interpicket H-bonding

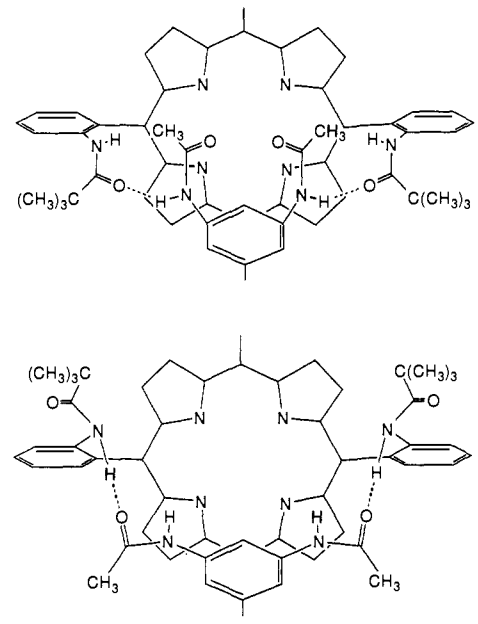

Figure 8. Alternate conformations for the 3,5-diacetamide ligand **10** showing possible interpicket H-bonding. The two conformations differ as to whether the acetamides act as donors or acceptors.

Table II. Kinetic Parameters and Equilibrium Constants for CO and O_2 Binding to Substituted Picket-Fence Iron(II) Porphyrins (Toluene, 25 °C, 1,2-Dimethylimidazole as Axial Base)

porphyrin	$10^{-5}k_{on}^{CO}$ (m^{-1} s^{-1})	$10^{-7}k_{on}^{O_2}$ (m^{-1} s^{-1})	$10^{-4}k_{off}^{O_2}$ (s^{-1})	$10^{-3}K^{O_2}$ (m^{-1})
picket-fence	15.9	21.6	5.6	3.9
indole **3**	15.5	24.0	2.4	10.0
benzofuran **5**	14.0	27.0	4.3	6.3
phenylurea **6**	3.9	3.8	0.1	34.5
3-phenol **8**	13.2	18.9	0.5 (77%)	37.8
			4.1 (23%)	4.6
3,5-diacetamide **10**	12.8	11.0	3.1 (65%)	3.5
			15.4 (35%)	0.7
3,5-methyl amide **12**	16.7	14.9	11.0	1.4

like that discovered in pincer porphyrin.[45] Space-filling models indicate that the 3- and/or 5-acetamide groups are capable of H-bonding to the amide groups of the adjacent pivalamide pickets as either donors or acceptors. This is illustrated in Figure 8. The third is rotation within the 3,5-acetamide groups themselves. There are, in fact, *16* different conformers possible in an all-planar 3,5-diacetamidophenyl moiety if all possible rotations around the C–N and N–(CO) bonds are considered. Given the simplicity of the variable-temperature spectrum of 3,5-diacetamidobenzoic acid, however, these conformational possibilities cannot be given much weight. Given the likelihood of both N–H tantomerism and interpicket H-bonding occurring with similar fluxionality barriers, it is not possible to unambiguously assign a unique rigid conformation to the superstructure of ligand **10** although its chemical purity is well established.

The three remaining ligands **11–13** all showed a single six-proton resonance in their room temperature spectra arising from their 3,5-substituted methyl groups. In the case of the 3,5-diacetate **11**, the variable-temperature spectrum was explored and the singlet was preserved throughout the range 233–333 K. Other changes were minor and consistent with the slight symmetry-lowering effect of frozen N–H porphyrin tautomers. The methyl singlet is consistent with either rapid rotation of the appended 3,5-disubstituted group about the amide linkage or alternatively with a structure having rigidly locked interpicket H-bonding of the type portrayed in Figure 8. The latter explanation actually seems more likely given the additivity of H-bonding to two adjacent pickets. The choice over the upper or lower possibilities in Figure 8 cannot be made for **10** and **12**. For the diacetate **11** and the dimethyl ester **13** only the lower structural type is possible since N–H moieties are only available in the pivalamide linkages. These conforma-

(48) Young, R.; Chang, C. K. *J. Am. Chem. Soc.* **1985**, *107*, 898.
(49) Odo, J.; Imai, H.; Kyuno, E.; Nakamoto, K. *J. Am. Chem. Soc.* **1988**, *110*, 742.
(50) Abraham, R. J.; Hawkes, G. E. *Tetrahedron Lett.* **1974**, 1483.
(51) Collman, J. P.; Brauman, J. I.; Iverson, B. L.; Sessler, J. L.; Morris, R. M.; Gibson, Q. H. *J. Am. Chem. Soc.* **1983**, *105*, 3052.
(52) Tagaki, S.; Miyamoto, T. K.; Sasaki, Y. *Bull. Chem. Soc. Jpn.* **1985**, *58*, 447.

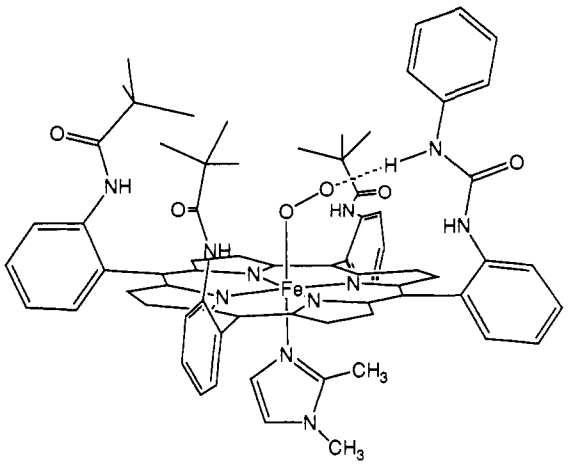

Figure 9. Proposed H-bonding to dioxygen in the complex of the phenylurea ligand **6**.

tional postulates led us to expect lower rather than higher oxygen affinities for these ligands since interpicket H-bonding removes polarity from deep in the $Fe(O_2)$ cavity and the conformations would appear to increase steric effects.

Dioxygen Affinities. The kinetic values used to determine the oxygen affinities for selected compounds are summarized in Table II. The close similarity of all of the rate parameters for the indole **3** and the benzofuran **5** suggests very close structural and electronic effects for these two substituents. This is consistent with the exo orientation of the indole N–H moiety deduced from NMR analysis (see Figure 6) because the nearby presence of a C–H bond on **3** and a lone pair on the oxygen atom of **5** do not present disparate dipole character to the FeO_2 moiety. The factor of 2 increase in the O_2 off rate and consequent decrease in O_2 affinity is probably too small for drawing firm conclusions, but is in the expected direction for dipolar *de*stabilization of the FeO_2 moiety by an opposing dipole at the furan oxygen.

The clearest demonstration of a distal effect on the O_2 affinity is provided by the phenylurea substituent in **6**. The 9-fold increase in affinity relative to picket-fence porphyrin is consistent with the positioning of the additional N–H of the urea group close the FeO_2 moiety, as deduced from the NMR analysis. We propose the formation of a H bond as illustrated in Figure 9. Such stabilization of the O_2 adduct is expected to be reflected predominantly in the off rate. Indeed, there is a ~50-fold decrease in $k_{off}^{O_2}$ relative to picket-fence porphyrin. A ~6-fold decrease in the corresponding on rate leads to the overall 9-fold effect on the affinity and suggests a destabilization of the transition state via a steric effect. This is also reflected in a 4-fold decrease in the CO on rate.

An effect similar to that seen in the phenylurea derivative is seen with the 3-phenol derivative **8**. A 10-fold decrease in $k_{off}^{O_2}$ relative to picket-fence porphyrin is consistent with H-bond stabilization of the dioxygen adduct by the phenolic proton. However, the compound has a very short lifetime compared to the phenylurea derivative, and the kinetic results are complicated by biphasic behavior. There is a minor component (23%) which shows comparable O_2 affinity to picket-fence porphyrin. These results mirror the lack of conformational rigidity suggested by the ^1H NMR of the free ligand. The same complication, of two components, arises with the 3,5-diacetamide **10**, and we have suggested[40] that O_2 binding on both sides of the porphyrin, giving spectroscopically indistinguishable (UV–vis) isomers, is the most likely rationale for these unexpected biphasic kinetics. The kinetic and equilibrium parameters of the final compound in Table II, the 3,5-methyl amide **12**, show no more than a 2-fold difference from picket-fence porphyrin. This is consistent with a ligand superstructure having interpicket H-bonding which effectively removes the methyl amide moiety from a close interaction with the coordinated dioxygen.

It is gratifying that the ligand structures, determined by NMR on the free-base porphyrins, agree so well with those implied by the properties of the oxygenated iron complexes. In many cases, the intraligand H-bonding which thwarts optimal orientation of the H-bonding donor cannot be overcome by the more modest energetics of H-bonding to the FeO_2 moiety.

Conclusions

The 9-fold increase in dioxygen affinity of the phenylurea derivative relative to picket-fence porphyrin illustrates a significant effect from adding a correctly oriented NH moiety to the superstructure. This corresponds to a free energy difference of 1.3 kcal/mol. The magnitude of the effect is quite small considering that hydrogen bonds frequently have free energies of formation of several kilocalories per mole. There are a number of possible explanations for the small contribution. The first is that the phenylurea may be restrained from optimal approach and orientation by the rigidity of the urea linkage and by bumping interactions with the *tert*-butyl groups of the neighboring pickets. We must await precise structural data to determine these details. A second possible factor is that the additional N–H interaction of the urea relative to an amide is not additive in absolute terms. The dipolar stabilization of dioxygen by the amide of a picket is not really replaced in the urea derivative. Rather, it is retained and augmented with an additional N–H group. The added N–H bond may "see" the terminal oxygen atom of the FeO_2 moiety as a diminished electron donor because of moderation by the preexisting FeO_2/amide dipole/dipole interaction. A third and more subtle possibility is that, for the phenylurea substituent, the solvent reorganization upon oxygenation contributes a more positive free energy than in the case of the pivalamide. This has been discussed in terms of solvent displacement in flat porphyrins[50] but should be a less significant factor in the present system. The 3-fold difference in O_2 affinity of picket-fence porphyrin and "tulip garden" porphyrin[50] (*tert*-butyl vs adamantyl) perhaps gives some idea of the maximum magnitude of this effect.

The 1.3 kcal/mol effect in the present work is thus seen to be a *minimum* estimate of the potential contribution to stabilization of dioxygen binding by a hydrogen bond. This is because an overall ΔG measurement is necessarily the summation of the effect of the added H bond minus the effect of other bonds that are broken or altered.

The overall magnitude of the effect is very similar to the ~ 10-fold diminution of the dioxygen affinity of myoglobin when the distal histidine is replaced by glycine or valine via site-directed mutagenesis.[9] It might be argued that this congruence is coincidental since replacement by phenylalanine leads to a 110-fold effect, i.e., 2.8 kcal/mol. However, in the absence of detailed structural information on each mutant, it is not possible to ascribe this effect simply to the addition of a distal histidine H bond. Ideally, one would like a mutation to replace a protein residue and leave the rest of the molecule completely unchanged. In reality, many subtle adjustments of structure are likely to occur. Water molecules may fill voids, dipoles may reorient, bulky replacement residues (e.g., phenylalanine) may inhibit O_2 binding, and the FeO_2 moiety may even change its angular orientation with respect to the $Fe–N_{porph}$ bonds. All of these structural adjustments will influence O_2 affinity. In doing so, these adjustments to a perturbation may conspire to thwart the effect of the nominal replacement. It does seem likely, at this stage of our understanding, that the absolute free energy contribution of a H bond to dioxygen binding may be underestimated in both models and proteins. On the other hand, it appears from the neutron diffraction study of oxymyoglobin that the N–H bond of the distal histidine is in fact restrained from optimal alignment for strong hydrogen bonding. It is not coplanar with the Fe–O–O moiety. Rather, it is positioned off to the side so that there is an oblique interaction with both the iron-bound O atom and the terminal O atom.[20] In mutant proteins, as well as in systematically substituted model compounds, the accumulation of precise structural data will be necessary to advance a legitimate partitioning of all of the effects that can influence dioxygen affinities. The good crystallizing tendencies of myoglobin and picket-fence-type model compounds suggests that such data may be forthcoming. In

addition, calculational approaches may offer corroborative structural and thermodynamic evidence.[53]

Acknowledgment. We thank Dr. Michel Momenteau for very helpful discussions and Dr. Masahiro Mikuriya for experimental assistance. This work was supported by National Institutes of Health Grant GM 23851.

(53) Lopez, M. A.; Kollman, P. A. *J. Am. Chem. Soc.* **1989**, *111*, 6212.

Supplementary Material Available: Figures S1-S12 showing ^{1}H NMR spectra at 270 MHz of compounds **2-13** (12 pages). Ordering information is given on any current masthead page.

Mechanism of Halide-Induced Disproportionation of $M(CO)_3(PCy_3)_2^+$ 17-Electron Radicals (M = Fe, Ru, Os). Periodic Trends on Reactivity and the Role of Ion Pairs

Lin Song and William C. Trogler*

Contribution from the Department of Chemistry, University of California, San Diego, La Jolla, California 92093-0506. *Received June 12, 1991*

Abstract: Halide-induced disproportionation of the 17-electron $M(CO)_3(PCy_3)_2^+$ radicals was probed by double potential step chronocoulometry, rotating-ring-disk electrochemistry, bulk coulometry, and cyclic voltammetry. The products of disproportionation, $M(CO)_3(PCy_3)_2$ and $MX_2(CO)_2(PCy_3)_2$, were observed directly for M = Ru and Os, and X = Cl^- or Br^-. At a constant concentration, $[Bu_4NPF_6]$ + $[Bu_4NX]$ = 0.2 M, the kinetics of disproportionation followed the rate law $k_2[Bu_4NX][M(CO)_3(PCy_3)_2PF_6]$. Conductivity measurements in the reaction solvent CH_2Cl_2 were fit to the Fuoss equation, and K_d, the dissociation constant for the ion pairs, ranged between 2.57×10^{-5} for $[Bu_4N]Cl$ and 4.26×10^{-5} for $[Bu_4N]PF_6$ at 25 °C. The $[Fe(CO)_3(PCy_3)_2]PF_6$ species has $K_d \approx 1.7 \times 10^{-4}$. Unlike 18-electron systems, the periodic effect on the reactivity of 17-electron $M(CO)_3(PCy_3)_2^+$ showed only a slight variation. For $[Bu_4N]Cl$ at 25 °C the rates k_2 were 66 M^{-1} s^{-1} (Fe), 280 M^{-1} s^{-1} (Ru), and 27 M^{-1} s^{-1} (Os). For $[Bu_4N]Br$ hardly any variation occurred along the series: 17 M^{-1} s^{-1} (Fe), 26 M^{-1} s^{-1} (Ru), and 20 M^{-1} s^{-1} (Os). The pseudo-first-order rate constants k_{obs} showed a nonlinear dependence on the concentration of the inert electrolyte $[Bu_4N]PF_6$, and are zero order in $[Bu_4N]X$ in the absence of $[Bu_4N]PF_6$. This data, however, fit well to a kinetic scheme that involved equilibration of contact ion pairs, followed by unimolecular substitution within the contact ion pair $\{[M(CO)_3(PCy_3)_2]X\}_{ip}$. The internal substitution rates and the equilibrium constants for ion pair exchange, measured at 25 °C, are as follows (k (s^{-1}), K): for $[Bu_4N]Cl$, 15 ± 3, 0.9 ± 0.2 (Fe), 56 ± 5, 0.79 ± 0.07 (Ru), 4.8 ± 0.9, 0.7 ± 0.1 (Os); for $[Bu_4N]Br$, 3.3 ± 0.1, 0.98 ± 0.03 (Fe), 5.5 ± 0.5, 1.02 ± 0.05 (Ru), 4.4 ± 0.7, 0.9 ± 0.1 (Os). Activation parameters obtained for $M(CO)_3(PCy_3)_2^+/Bu_4NCl$ systems are as follows ($\Delta H^\ddagger$ (kcal mol^{-1}), $\Delta S^\ddagger$ (cal mol^{-1} K^{-1})): 19.7 ± 0.9, 10 ± 3 (Fe); 18.7 ± 1.6, 12 ± 5 (Ru); 12.1 ± 0.7, −14 ± 3 (Os).

Introduction

For 17-electron organometallic radicals the bulk of experimental evidence supports an associative mechanism for ligand substitution reactions.[1] A 19-electron intermediate or transition state, stabilized by metal-nucleophile σ-bonding, has been proposed[1,2] to explain the 10^9-10^{10} increase in ligand substitution rates observed[3] in comparison to analogous 18-electron complexes. One question, which remains unanswered, is the periodic effect on reactivity of 17-electron radicals. In mononuclear 18-electron complexes an enhanced reactivity occurs for second-row transition metals.[4] For example, in the iron triad[5] the relative labilities of $M(CO)_5$ complexes toward CO substitution follow the order Fe (1) < Os (800) < Ru (5×10^7). Rate data for $Fe(CO)_4(PPh_3)$[6] and $Ru(CO)_4(PPh_3)$[7] again show a 10^8 increase in reactivity for the Ru complex.

Previously we examined[3b] the disproportionation of a series of $Fe(CO)_3L_2^+$ 17-electron complexes (L = organophosphine ligand) induced by various substituted pyridine nucleophiles. This paper includes the generation of Ru and Os analogues for mechanistic comparison. Because these latter compounds are unreactive toward pyridine nucleophiles, $[NBu_4]Cl$ and $[NBu_4]Br$ nucleophiles had to be used for the complete triad. Halide ions were known[8] to cause disproportionation for $Fe(CO)_3(PPh_3)_2^+$. An additional interesting question about the role of ion pairs vs free ions arose in the study of this reaction mechanism. Ion pairing of charged organometallic compounds has been observed spectroscopically for many systems in solvents of low dielectric constant.[9,10] The most common examples involve salts of carbonylmetalates. For example, Kochi's work[10] clearly establishes the importance of contact ion pair equilibria on the photochemistry of organometallic charge-transfer complexes. The study described here for carbonylmetal cations suggests a crucial role for ion pairing in their

(1) (a) Tyler, D. R. *Prog. Inorg. Chem.* **1988**, *36*, 125. (b) Trogler, W. C. In *Organometallic Radical Processes*; Trogler, W. C., Ed.; Elsevier: Amsterdam, 1990; pp 306-337.
(2) Therien, M. J.; Trogler, W. C. *J. Am. Chem. Soc.* **1988**, *110*, 4942.
(3) (a) Shi, Q.-Z.; Richmond, T. G.; Trogler, W. C.; Basolo, F. *J. Am. Chem. Soc.* **1984**, *106*, 71. (b) Therien, M. J.; Ni, C.-L.; Anson, F. C.; Osteryoung, J. G.; Trogler, W. C. *J. Am. Chem. Soc.* **1986**, *108*, 4037.
(4) (a) Basolo, F.; Pearson, R. C. *Mechanisms of Inorganic Reactions*, 2nd ed.; Wiley: New York, 1967; p 576. (b) Atwood, J. D. *Inorganic and Organometallic Reaction Mechanisms*; Brooks/Cole Publ.: Monterey, CA, 1985; pp 108-111.
(5) Shen, J.-K.; Gao, Y.-C.; Shi, Q.-Z.; Basolo, F. *Inorg. Chem.* **1989**, *28*, 4304.
(6) Siefert, E. E.; Angelici, R. J. *J. Organomet. Chem.* **1967**, *8*, 374.
(7) Johnson, B. F. G.; Lewis, J.; Twigg, M. V. *J. Chem. Soc., Dalton Trans.* **1975**, 1876.
(8) Baker, P. K.; Connelly, N. G.; Jones, B. M. R.; Maher, J. P.; Somers, K. R. *J. Chem. Soc., Dalton Trans.* **1980**, 579.
(9) Darensbourg, M. Y.; Ash, C. E. *Adv. Organomet. Chem.* **1987**, *27*, 1.
(10) Kochi, J. K. In *Organometallic Radical Processes*; Trogler, W. C., Ed.; Elsevier: Amsterdam, 1990; pp 201-269.

0002-7863/92/1514-3355$03.00/0